Performance of shielded electromagnet - evaluation under low frequency excitation

Gael Bringout, *Member, IEEE* and Ksenija Gräfe and Thorsten M. Buzug, *Member, IEEE*

Methods to evaluate the eddy current amplitude induced in a shield are presented. This is used to asses the effect of those currents on the efficiency of coils in an MPI scanner. The example of a shielded drive coil is introduced and a finite element method and a boundary element method are used to evaluate the loss of efficiency of the coil when operated with AC signals. The calculation needed to implement the boundary element method are detailed, which offer an analytic representation of the phenomena. This, in turn, improves the available knowledge to make design decision at the scanner level. Results of both methods are found to be similar, when the field generated by a coil with different shields are compared. However, the calculation cost of the boundary element method is far inferior. The boundary element method calculation shows that, besides the used frequency, the geometry of the system, and the shielding material, there is little to be done in order to increase the shielded-coil performance. In addition, the results for this methods may be integrated into an optimization scheme in order to integrate them for the design of coils.

***Index Terms*—MPI, electromagnet design, boundary element method, finite element method, shielding, eddy current.**

I. Introduction

MAGNETIC particle imaging (MPI) is an imaging technique to visualize a volume containing a distribution of magnetic nanoparticles [1]. First *in vivo* experiments performed with mice have demonstrated that this technique is able to acquire data with high sensitivity, high resolution, and high speed [2], [3].

In order to reach this high speed, magnetic fields varying continuously in time with a sinusoidal shape are commonly used. Also, MPI scanners use low inductance, high voltage coils to generate the drive fields and high inductance, low voltage coils to generate the selection fields. Therefore, a coupling between the drive coils and the selection coils would result in a high voltage peak on the selection coils, which may have a too high amplitude to be absorbed by the coils without damage. If the coupling factor between the coils is not negligible, it would be preferred to shield the selection coils against the high frequency fields. Moreover, if the selection coils are not made of litz wire, the used material is likely to behave as shield for the high frequencies fields. For those reason, the effects of induced eddy current in a shield due to the time variation of the signal have to be investigated.

Due to the induced current in the shield, the field topologies may be changed. This is of little influence for field free point scanners, but for scanners using a field free line, the influence may be of greater importance as the line properties strongly depend on the field topology.

Finally, the efficiency of the coil will be effectively reduced, which means that for a given peak current amplitude, the field amplitude generated by the system coil and shield will be reduced. A shielded-coil will require more current as an unshielded one to produce the same field amplitude. Additionally to the reduced efficiency, the power dissipated by the shield will be provided by the drive coil power supply, whereas the stored energy (and thus, the inductance of the drive coil) will be reduced. The cooling and the electrical resistance of the coil should therefore be planned accordingly.

To be able to quantify the effect of the shield on the coil performance, some analytical formulas exist for the increase of the resistance and the reduction of the inductance [4]. Those formulas are sufficient for simple geometries, but they do neither permit the calculation of the loss in efficiency nor the change in field topology. To be able to accurately do so, we propose to use the boundary element method (BEM). This method is chosen to achieve two goals. The first is the reduction of the simulation cost and error, as BEM better handles volumetric quantities in comparison to the finite element method (FEM). The second is the availability of the induced current into the shield for further optimization with the BEM formulation [5].

In this paper, the BEM formulation of the induced current in a target volume by a sinusoidally varying current on a source volume is developed. The FEM is used to validate the results of the BEM simulation using the field amplitudes generated by two equivalent systems. Finally, the change in topology of the magnetic field is assessed.

II. Methods

In the first section, the BEM model is explained and the extension regarding the induced current is detailed. Then, a description of the FEM model is given.

A. Boundary element method

BEM uses the meshed surfaces S_s and S_i to model the surfaces of the coil (S_s as source surface, where the current density is directly applied) and the shield (S_i carrying an induced current density), respectively [5]–[7].

1) Basics - quasi-static model

To represent the current density $j(\mathbf{r})$ with $\mathbf{r} \in S_\mathrm{i} \cup S_\mathrm{s}$ a stream functions $\psi(\mathbf{r})$ is used

$$\mathbf{j}(\mathbf{r}) = \mathrm{curl}(\psi(\mathbf{r})\mathbf{n}(\mathbf{r})). \tag{1}$$

G. Bringout K. Gräfe and T. M. Buzug are with the Institute of Medical Engineering, Universität zu Lübeck, Lübeck, Germany. e-mail: {bringout,buzug}@imt.uni-luebeck.de.

Manuscript received xxxxx xx, xxxx; revised xxxxx xx, xxxx.

The stream function is expressed on meshes of $N = N_\mathrm{s} + N_\mathrm{i}$ nodes in a finite set of basis stream function $\widehat{\psi}(\mathbf{r})$,

$$\psi(\mathbf{r}) = \sum_{n=1}^{N} s_n \widehat{\psi}_n(\mathbf{r}), \tag{2}$$

with s_n the stream function amplitude at position $\mathbf{r}$, N_s and N_i the number of nodes of the mesh of S_s and S_i, respectively. The vector $\mathbf{s} = [s_1 \ s_2 \ \dots \ s_N]^\intercal$ therefore models the current density on the meshes. This vector can also be partitioned to reflect the separation of the meshes with

$$\mathbf{s} = \begin{bmatrix} \mathbf{s}_\mathrm{s} \\ \mathbf{s}_\mathrm{i} \end{bmatrix}. \tag{3}$$

The mutual inductance matrix $\mathbf{M}$ and resistance matrix $\mathbf{R}$ [5] associated to the meshes can also be partitioned as

$$\mathbf{M} = \begin{bmatrix} \mathbf{M}_\mathrm{s} & \mathbf{M}_\mathrm{si} \\ \mathbf{M}_\mathrm{is} & \mathbf{M}_\mathrm{i} \end{bmatrix} \text{ and } \mathbf{R} = \begin{bmatrix} \mathbf{R}_\mathrm{s} & 0 \\ 0 & \mathbf{R}_\mathrm{i} \end{bmatrix}. \tag{4}$$

Here, $\mathbf{M}_\mathrm{s}$ and $\mathbf{R}_\mathrm{s}$ are the mutual inductance and resistance, respectively, associated to the surface S_s. $\mathbf{M}_\mathrm{i}$ and $\mathbf{R}_\mathrm{i}$ are the ones associated to the surface S_i. Finally, $\mathbf{M}_\mathrm{si}$ is the mutual inductance between the meshes S_s and S_i and $\mathbf{M}_\mathrm{is} = \mathbf{M}_\mathrm{si}^\intercal$. The matrices $\mathbf{M}_\mathrm{is}$ and $\mathbf{M}_\mathrm{i}$ are symmetric, positive definite and square. Matrix $\mathbf{R}_\mathrm{i}$ is symmetric, positive semi-definite and square.

2) Time varying correction

To model the time variation of the fields in a representative way for MPI scanners, the example of a drive coil is taken. Those coils are often used with a sinusoidal signal

$$\mathbf{s}_\mathrm{s}(t) = \mathbf{s}_\mathrm{s} \sin(\omega t), \tag{5}$$

with the angular frequency $\omega = 2\pi f$, with f the signal frequency.

The time varying functions $\mathbf{s}_\mathrm{i}(t)$ will then depend on $\mathbf{s}_\mathrm{s}(t)$, $\mathbf{M}_\mathrm{is}$, $\mathbf{M}_\mathrm{i}$ and $\mathbf{R}_\mathrm{i}$ following the law of conservation of energy [6] as

$$\mathbf{M}_\mathrm{is}\frac{d\mathbf{s}_\mathrm{s}}{dt} + \mathbf{M}_\mathrm{i}\frac{d\mathbf{s}_\mathrm{i}}{dt} + \mathbf{R}_\mathrm{i}\mathbf{s}_\mathrm{i} = 0. \tag{6}$$

This relation describes the voltage across the mutual inductance of the two meshes due to the source current as the opposite of the sum of the voltage across the inductance of the shield and the voltage across the electrical resistance of the shield.

The equation (6) can be rewritten as a standard differential equation

$$\mathbf{M}_\mathrm{i}\frac{d\mathbf{s}_\mathrm{i}}{dt} = -\mathbf{R}_\mathrm{i}\mathbf{s}_\mathrm{i} - \mathbf{M}_\mathrm{is}\frac{d\mathbf{s}_\mathrm{s}}{dt}, \tag{7}$$

thus

$$\frac{d\mathbf{s}_\mathrm{i}}{dt} = -\mathbf{M}_\mathrm{i}^{-1}\mathbf{R}_\mathrm{i}\mathbf{s}_\mathrm{i} - \mathbf{M}_\mathrm{i}^{-1}\mathbf{M}_\mathrm{is}\frac{d\mathbf{s}_\mathrm{s}}{dt}. \tag{8}$$

3) Solving the differential equation

In order to solve (8), the matrix $\mathbf{M}_\mathrm{i}^{-1}\mathbf{R}_\mathrm{i}$ is diagonalized, using the relation

$$\mathbf{M}_\mathrm{i}^{-1}\mathbf{R}_\mathrm{i} = \mathbf{Q}\mathbf{\Lambda}\mathbf{Q}^{-1}, \tag{9}$$

with $\mathbf{Q}$ the matrix formed by the eigenvectors and $\mathbf{\Lambda}$ the diagonal matrix formed with the eigenvalues λ.

Equation (8) can be rewritten, taking into account the relation (9), as

$$\frac{d\mathbf{s}_\mathrm{i}}{dt} = -\mathbf{Q}\mathbf{\Lambda}\mathbf{Q}^{-1}\mathbf{s}_\mathrm{i} - \mathbf{M}_\mathrm{i}^{-1}\mathbf{M}_\mathrm{is}\frac{d\mathbf{s}_\mathrm{s}}{dt}, \tag{10}$$

$$\mathbf{Q}^{-1}\frac{d\mathbf{s}_\mathrm{i}}{dt} = -\mathbf{\Lambda}\mathbf{Q}^{-1}\mathbf{s}_\mathrm{i} - \mathbf{Q}^{-1}\mathbf{M}_\mathrm{i}^{-1}\mathbf{M}_\mathrm{is}\frac{d\mathbf{s}_\mathrm{s}}{dt}. \tag{11}$$

The variable $\mathbf{Q}^{-1}\mathbf{s}_\mathrm{i}$ can be substituted by $\mathbf{y}_\mathrm{i}$, and the product $-\mathbf{Q}^{-1}\mathbf{M}_\mathrm{i}^{-1}\mathbf{M}_\mathrm{is}$ can be replaced by the matrix $\mathbf{P}$, which leads to

$$\frac{d\mathbf{y}_\mathrm{i}}{dt} = -\mathbf{\Lambda}\mathbf{y}_\mathrm{i} + \mathbf{P}\frac{d\mathbf{s}_\mathrm{s}}{dt}. \tag{12}$$

Using the variation of parameters, a solution to (12) can be found as

$$\mathbf{y}_\mathrm{i}(t) = e^{-\mathbf{\Lambda}t}\mathbf{y}_\mathrm{i}(t_0) + e^{-\mathbf{\Lambda}t}\int_{t_0}^{t} e^{\mathbf{\Lambda}\tau} + \mathbf{P}\frac{d\mathbf{s}_\mathrm{s}}{d\tau}d\tau, \tag{13}$$

with t_0 the time at which the current starts to flow in the coil. Using the $\mathbf{s}_\mathrm{i}$ variable, (13) can be written as

$$\begin{aligned}\mathbf{s}_\mathrm{i}(t) &= \mathbf{Q}e^{-\mathbf{\Lambda}t}\mathbf{Q}^{-1}\mathbf{s}_\mathrm{i}(t_0) \\ &+\mathbf{Q}e^{-\mathbf{\Lambda}t}\int_{t_0}^{t} e^{\mathbf{\Lambda}\tau} + \mathbf{P}\frac{d\mathbf{s}_\mathrm{s}(\tau)}{d\tau}d\tau.\end{aligned} \tag{14}$$

Assuming that the current density in the shield at $t_0 = 0$ is zero, replacing the relation (5) into (14) leads to

$$\mathbf{s}_\mathrm{i}(t) = \mathbf{Q}\int_0^t e^{-\mathbf{\Lambda}(t-\tau)}\frac{d\sin(\omega\,\tau)}{d\tau}d\tau\,\mathbf{P}\mathbf{s}_\mathrm{s}. \tag{15}$$

4) Simplification

We can define, for $k = 1, ..., N_\mathrm{i}, t \geq t_0$,

$$a_k(t) = \int_0^t e^{-\lambda_k(t-\tau)}\frac{d\sin(\omega\ \tau)}{d\tau}d\tau, \tag{16}$$

which is equivalent to

$$a_k(t) = \frac{-\omega\lambda_k e^{-\lambda_k t}}{\omega^2 + \lambda_k^2} \tag{17}$$

$$+\frac{\omega\lambda_k\cos(\omega t)}{\omega^2 + \lambda_k^2} \tag{18}$$

$$+\frac{\omega^2\sin(\omega t)}{\omega^2 + \lambda_k^2}. \tag{19}$$

Equation (15) can then be simply rewritten as

$$\mathbf{s}_\mathrm{i}(t) = \mathbf{Q}\ \mathrm{diag}(a_1(t), ..., a_{N_\mathrm{i}}(t))\,\mathbf{P}\mathbf{s}_\mathrm{s}. \tag{20}$$

It has to be noted that, after a few periods, the term (17) can be neglected and thus $\mathbf{s}_\mathrm{i}(t)$ can be expressed as

$$\mathbf{s}_\mathrm{i}(t) = \mathbf{s}_\mathrm{iCos}\cos(\omega t) + \mathbf{s}_\mathrm{iSin}\sin(\omega t), \tag{21}$$

with

$$\mathbf{s}_\mathrm{iCos} = \mathbf{Q}\ \mathrm{diag}(\frac{\omega\lambda_1}{\omega^2 + \lambda_1^2}, ..., \frac{\omega\lambda_{N_\mathrm{i}}}{\omega^2 + \lambda_{N_\mathrm{i}^2}})\,\mathbf{P}\mathbf{s}_\mathrm{s}, \tag{22}$$

$$\mathbf{s}_\mathrm{iSin} = \mathbf{Q}\ \mathrm{diag}(\frac{\omega^2}{\omega^2 + \lambda_1^2}, ..., \frac{\omega^2}{\omega^2 + \lambda_{N_\mathrm{i}^2}})\,\mathbf{P}\mathbf{s}_\mathrm{s}. \tag{23}$$

Thus, in the shield will flow a time dependent current density, having sine and cosine components. The used implementation is available on http://www.imt.uni-luebeck.de and http://github.com/gBringout/CoilDesign.

B. Finite element method

The calculation software COMSOL Multiphysics® was used to simulate the field generated in the middle of an assembly composed by a drive coil and a shield.

1) Geometry definition

The design of the coils was obtained using a BEM framework [5]. In order to model the coil, a high resolution cylindrical mesh was set as surface and a drive coil was designed with set constraints. The centroids obtained with these methods are connected to form a wire path using a CAD software and the wire section is then swept along the wire path to form the conductor volume, as shown in Fig 4 (a) to (b). The shield is modeled as a hollow cylinder.

2) Definition of materials

The conductor is modeled as an electrical conductor with a very low electrical conductivity to simulate the behaviour of an ideal litz wire. The shield is modeled as an homogeneous copper cylinder.

3) Meshing

The main mesh constraint is given by the resolution needed to resolve the induced current in the shield. The mesh size across this thin cylinder should be at least equal to the skin depth for a few elements. We used 3 elements with a 0.30 mm thickness, knowing that a 0.42 mm skin depth is expected in a copper cylinder subjected to a 25 kHz signal.

4) Solving

The setup problem is then solved in the frequency domain using the default parameter and solver.

C. Magnetic field density evaluation

As the considered coil is used to generate fields mainly in the y direction, all the magnetic field values will refer to the y components of the magnetic field density vector. To minimize the error due to the magnetic field density evaluation, both results are post-processed in the same way. The fields are expressed as a spherical harmonics series expansion [8], which enables a precise description of the field topology. The 0^{th} degree coefficient of the field is calculated, using an expansion of 6^{th} order. This coefficient is used for the calculation of the coil efficiency.

As equation (20) shows, the field generated by the shield is directly proportional to $\mathbf{s}_\text{s}$. Thus, the peak field amplitude generated by the system coil and shield at a given frequency is expressed as the ratio ν multiplied by the field amplitude generated by the system under a DC signal. That is

$$B_{\text{frequency}} = \nu\, B_{\text{DC}}, \tag{24}$$

for a given frequency. A frequency of 25 kHz will be taken as example for both methods.

III. Results

The 0^{th} degree coefficient of the field has been evaluated for a coil producing a with a mean radius of 0.119 m and a length of 0.250 m surrounded by a 2 mm thick copper shield with a mean radius varying from 0.135 m to 0.220 m and a length of 0.4 m. The coil and the shield are always arranged in a concentric and symmetric way. The field ratio ν has been calculated for each method and is shown in Fig.1. Selected spherical harmonics coefficients from the BEM simulation are shown in Fig. 2.

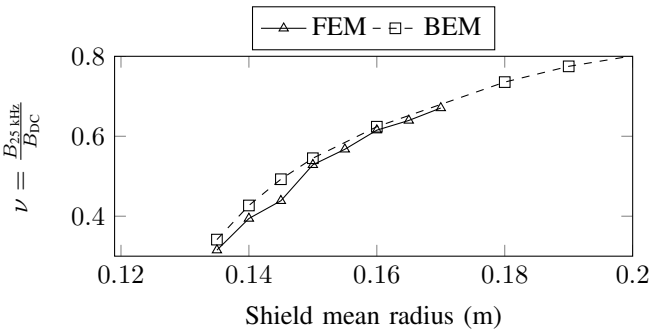

Fig. 1. Comparison of the calculation results via FEM and BEM calculations.

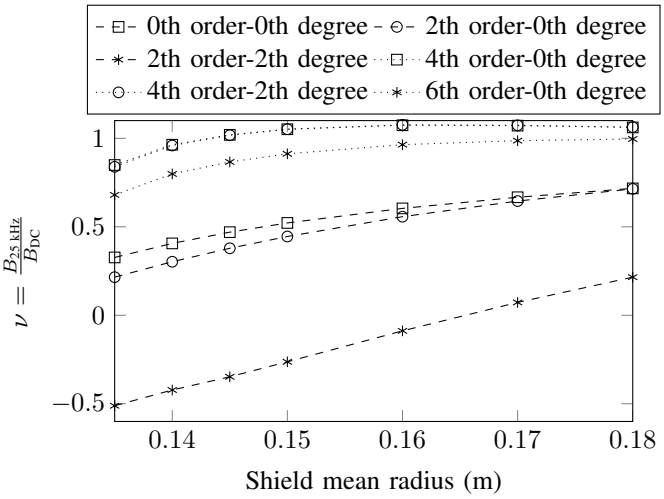

Fig. 2. Comparison of the spherical harmonics coefficients having an absolute value higher than 0.2 mT in B_{DC} for a target field of 15 mT from the BEM simulation. The field topology is slightly changed with change in shield diameter.

A. Boundary element method

The shield and the coil are modeled as coarse meshed surfaces made of 440 and 420 nodes, respectively. It has to be noted, that the cosine term (18) is smaller than the sine term (19). Indeed, the biggest λ_k is of the order 10^2 and ω is in the order of 10^5. The field generated by the shield is thus dephased by 180° to the field generated by the coil. This means that the field generated by the shield will be subtracted from the one generated by the coil. The stream function amplitudes s_s and s_i are displayed in Fig. 3. The calculation from loading the mesh to calculating the 0^{th} degree coefficient took 286 seconds on an Intel Core i5 760 CPU and required around 160 MB of memory using a Matlab implementation of the method under Windows.

B. Finite element method

The coil modeled in 3D is imported into the software and the rest of the geometry is defined inside the software, as

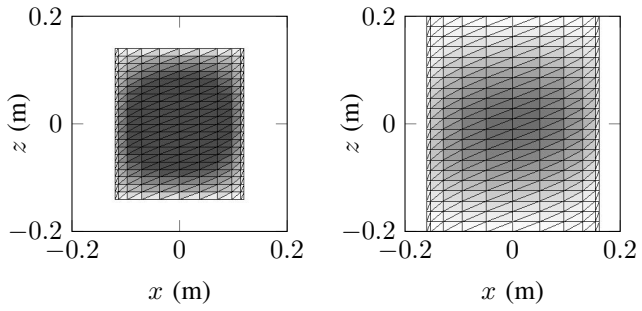

Fig. 3. Top views of the stream function amplitude on the meshed surfaces for the coil (a) and for the shield (b). The grey values show the stream function amplitude on the same scale.

shown in Fig. 4. To reduce the number of nodes needed to model the system, the meshing resolution of the shield is kept optimal for each area. This means that in the area where induced currents are expected, the node density is increased in the shield thickness, but not in the shield length. The 0.4 mm thin elements needed for the calculation of the induced current are thus several millimeters long, leading to some errors and limitations. Despite this approximation, the calculation of the current density and the fields took 913 seconds on an Intel Core i5 760 CPU and required around 12 GB of memory per shield radius.

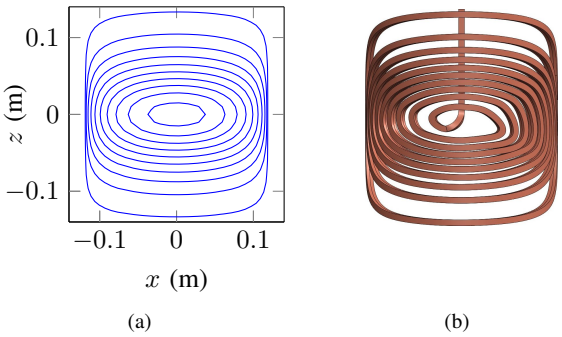

Fig. 4. Required data to build the FEM model. (a) The centroids of the ideal current density are calculated. (b) In a CAD software, the centroids are connected to create a current path. A section is swept along this current path to create the coil model. It is then imported into the FEM software and the rest of the geometry is done using the integrated geometry elements.

IV. Discussion

The field reduction calculated with the two methods in Fig. 1 are in good accordance with the FEM results, thus validating our BEM simulation. The rough FEM curve may come from the relatively bad quality of the mesh, which depend on the radius of the shield.

It can be noted that the efficiency loss of the shielded coil is important for the chosen shield diameter. Half of the efficiency is lost when the shield is placed 26 mm away of the coil centroid. This means that to generate the same field amplitude as calculated for the DC current, the peak current has to be increased by a factor of 2. The dissipated heat in the coil will be then increased by a factor of $(2/\sqrt{2})^2 = 2$ compared to the DC case. Moreover, the induced energy in the shield will have to be provided by the coil power supply. This power will be dissipated as heat in the shield, which may require an active cooling to be maintained at an acceptable temperature.

Fig. 2 shows that the field topology is slightly modified by the changes in the shield radius, as the components ratios do not all follow the same curve. But it has to be kept in mind that the spherical harmonics coefficients of order higher than 0 have an amplitude which is at least 5 times smaller than the 0^{th} order coefficient, thus limiting the actual topology change. The actual effect on the line shape has still to be investigated.

In order to better control the field topology and the efficiency loss, the presented passive shield may be replaced or assisted by a coil reducing the unwanted field, which is often referred to as an active shield in the literature.

V. Conclusion

The presented BEM simulation permits quick and precise calculation of the magnetic field density generated by the induced current in a shield. Moreover, (20) gives an insight on how to influence the amplitude of this field. The distance between the coil and the shield, the selection of the drive frequency and the selection of the shield material are the main parameters, which can be adjusted in order to minimize the destruction of the drive field by the field generated by the induced current.

Those results offer the possibility to improve scanner design by integrating the effect of time-varying current to pure quasi-static simulations. A trade-off between scanner size and drive coil efficiency should be studied in order to find the best compromise during the design phase of the scanner.

Finally, the precise required field topology for an FFL scanner should be defined, in order to asses the effect of the magnetic field topology changes on the imaging process. This may also help the design of future drive coils, active shields and shimming coils.

Acknowledgment

The authors gratefully acknowledge the support of the German Federal Ministry of Education and Research (BMBF) under grant number 13N11090 and of the European Union and the State Schleswig-Holstein with the Program for the Future-Economy under grant number 122-10-004.

References

[1] B. Gleich and J. Weizenecker, "Tomographic imaging using the nonlinear response of magnetic particles," *Nature*, vol. 435, no. 7046, pp. 1214–1217, 2005.

[2] J. Weizenecker, B. Gleich *et al.*, "Three-dimensional real-time in vivo magnetic particle imaging," *Physics in medicine and biology*, vol. 54, no. 5, p. L1, 2009.

[3] T. M. Buzug, G. Bringout *et al.*, "Magnetic particle imaging: Introduction to imaging and hardware realization," *Zeitschrift für Medizinische Physik*, vol. 22, no. 4, pp. 323 – 334, 2012.

[4] F. E. Terman, *Radio engineers' handbook*. McGraw-Hill New York, 1943, vol. 19.

[5] G. Bringout and T. M. Buzug, "Coil design for magnetic particle imaging: Application for a pre-clinical scanner," *Magnetics, IEEE Transactions on*, 2014.

[6] G. N. Peeren, "Stream function approach for determining optimal surface currents," Ph.D. dissertation, Technische Universiteit Eindhoven, 2003.

[7] M. Poole, "Improved equipment and techniques for dynamic shimming in high field mri," Ph.D. dissertation, The University of Nottingham, 2007.
[8] D. Winch, D. Ivers *et al.*, "Geomagnetism and schmidt quasi-normalization," *Geophysical Journal International*, vol. 160, no. 2, pp. 487–504, 2005.